Design of Aero-Engine Internal Model Control System Based on Neural Network Time-Delay Prediction

DU Xian[1,2]，MA Yan-hua[2,3]，WANG Xin-yue[4]，XU Ling[1]

（1. School of Control Science and Engineering，Dalian University of Technology，Dalian 116024，China；
2. Key Laboratory of Intelligent Control and Optimization for Industrial Equipment，Ministry of Education，Dalian University of Technology，Dalian 116024，China；
3. School of Microelectronics，Dalian University of Technology，Dalian 116024，China；
4. Beijing Power Machinery Institute，Beijing 100074，China）

Abstract：Aiming at the uncertainty of time-delay in aero-engine distributed control system，an internal model multi-variable control system based on neural network time-delay prediction is proposed for the aero-engine control. Firstly，the causes and influencing factors of the network-induced time-delay in distributed control system are investigated. Then the internal model controller with time-delay is designed，which includes the delay prediction module based on neural network，the main internal model controller module，the actuator inner-loop control module，and the switching control module that combined with the open-loop control plan for the engine starting process. The system stability performance of internal model control with time-delay prediction is analyzed theoretically under ideal and disturbance conditions，as well as the permitted time-delay is then explained under the proposed control strategy. Finally，the full digital simulation and hardware-in-the-loop tests are carried out. The results show that the designed neural network delay prediction module owns the ability to predict current time-delay in high-precision，and the steady-state error of the internal model controller is less than 0.5%. In addition，the proposed controller has satisfactory anti-interference performance and meets the real-time requirements，which has the feasibility of engineering application.

Key words：Aero-engine control；Neural network delay prediction；Internal model control；Multi-variable control；Hardware-in-the-loop simulation

CLC number：V233.7　**Document code**：A　**Article number**：1001-4055（2023）11-210903-13

DOI：10.13675/j.cnki. tjjs. 210903

基于神经网络时延预测的航空发动机内模控制器设计 *

杜　宪[1,2]，马艳华[2,3]，王欣悦[4]，徐　羚[1]

（1. 大连理工大学 控制科学与工程学院，辽宁 大连 116024；
2. 大连理工大学 工业装备智能控制与优化教育部重点实验室，辽宁 大连 116024；
3. 大连理工大学 微电子学院，辽宁 大连 116024；
4. 北京动力机械研究所，北京 100074）

摘　要：针对航空发动机分布式控制系统中时延不确定问题，提出了一种基于神经网络时延预测的

* **收稿日期**：2021-12-27；**修订日期**：2022-03-29。
基金项目：国家自然科学基金（61903059；61903061；61890924）；航空科学基金（2019ZB063001）；辽宁省兴辽英才计划项目（XLYC1907070）；中央高校基本科研业务费（DUT22QN204）；国家科技重大专项（J2019-I-0019-0018）。
作者简介：杜　宪，博士，副教授，研究领域为航空发动机控制系统设计及应用。
通讯作者：马艳华，博士，副教授，研究领域为航空发动机控制与故障诊断。E-mail：mayanhua@dlut.edu.cn
引用格式：杜　宪，马艳华，王欣悦，等. 基于神经网络时延预测的航空发动机内模控制器设计[J]. 推进技术，2023，44（11）：210903. （DU Xian，MA Yan-hua，WANG Xin-yue，et al. Design of Aero-Engine Internal Model Control System Based on Neural Network Time-Delay Prediction[J]. *Journal of Propulsion Technology*，2023，44（11）：210903.）

航空发动机内模多变量控制设计方法。首先分析了分布式控制架构下网络时延产生的原因及影响因素。然后设计了内模控制器，包括基于神经网络的时延预测模块、内模主控制器模块、执行机构小闭环控制模块以及与发动机起动过程开环控制计划相结合的切换控制模块。在理想和扰动条件下，从理论上分析了基于预测时延的内模控制系统的稳定性能，并对所提控制策略下允许的最大时延进行了说明。最后进行了全数字仿真和硬件在环仿真试验。结果表明，所设计的神经网络时延预测模块具备高精度预测能力，内模控制器的稳态误差不超过0.5%，具有良好的抗干扰能力、并满足实时性要求，具有一定的工程应用价值。

关键词：航空发动机控制；神经网络时延预测；内模控制；多变量控制；硬件在环仿真

1 Introduction

With the intelligent improvement of aero-engine control requirements, the traditional centralized control architecture has been difficult to meet the complex control tasks. In order to further improve engine performance, aero-engine control system is gradually transitioning from centralized control architecture to distributed control architecture, due to its advantages of light weight, high reliability and low maintenance cost[1-2].

Although the distributed control system (DCS) has been considered as an important direction of future intelligent aviation power, the time-delay caused by distributed system in abnormal condition will affect the safety of the aero-engine[3]. This is because the existence of time-delay directly affects the signal transmission. If the control signals from the controller and the signals collected by the sensors cannot be sent to the corresponding node in time, the control performance of the system will be worsen. In addition, the time-delay characteristics of distributed control system inevitably lead to the complexity of the control system[4]. On one hand, the characteristic equations of infinite-dimensional systems are generally transcendental equations that are difficult to solve. On the other hand, based on classical control theory, the situation that the control effect deteriorates and even becomes unstable in the presence of time-delay may occur[5]. Therefore, the solution of time-delay problem is one of the key issues related to the application of distributed control.

At present, robust control methods such as state feedback and output feedback have become powerful tools for time-delay system control. Yedavalli et al.[6] analyzed robust stability for uncertain sampling time-delay systems, gave a stability criterion under uncertain time-delay, and designed a robust controller for a turbine engine with given time-delay parameters. Belapurkar and Yedavall et al.[7-9] designed a distributed full authority digital engine control (Decentralized Distributed FADEC, D2FADEC) system based on a decentralized architecture. They carried out a research about the stability under time-delay and packet loss, and used the concept of packet loss margin (PDM) to describe the robustness of the control system in the case of packet loss. Kratz et al.[10] designed a robust full-state feedback fan speed control system with the goal of maximizing the stability margin during instantaneous packet loss. Jonathan and Belapurkar et al.[11-12] applied robust control techniques to the linear models of the T700 turbo-shaft engine and the C-MAPSS40K engine, in order to solve the network time-delay and packet loss problems in distributed control systems. In 2017, Seitz et al.[13] proposed two new structural robust stability bounds, to improve multi-delay modeling techniques, and a control logic based on dynamic compensators and state estimators, to enhance the robust stability bounds. However, the research on aero-engine time-delay system mostly stays in the traditional uni-variate control, and most of them only consider fixed time-delay, lacking the investigations on time-varying time-delay and ultra-long time-delay[14-15].

Internal model control (IMC) was first proposed by Garcia and Morari[16] in 1982, and improved on the basis of Smith predictor, which greatly enhanced the robustness of the control system. At the same time, internal model control is widely used in the field of time-delay system control because of its simple structure, small on-line adjustment parameters, strong anti-interference and good control effect for large time-delay systems[17-18]. Therefore, the aero-engine internal model control strategy is preferred in view of the existence of time-delay. On this basis, considering the uncertainty of the actual system time-delay, neural network[19-20] time-delay prediction method is then introduced, and thus the internal model control system based on time-delay prediction is proposed for the aero-engine control.

2 Aero-engine control scheme with time-delay

2.1 Time-delay analysis under distributed architecture

In a distributed control system, multiple intelligent nodes share a communication line, and each intelligent node needs to abide by the bus scheduling mechanism, and can occupy the bus for data transmission when the bus is idle and allowed to access. When the bus bandwidth is fixed, the waiting time for each node to compete for the bus will be prolonged with the increase of the number of nodes, which leads to non-negligible network time-delay, also known as network-induced time-delay. At the same time, due to the variety of data transmission paths in DCS, data packet loss and confusion occur from time to time, which will also cause network time-delay and further increase the uncertainty of the system.

The existence of network-induced time-delay makes the future states of the control system not only related to the current states, but also related to the past states. In the field of network control, such systems with network delay are called time-delay systems[21].

The time-delay composition of typical distributed control system is shown in Fig. 1. It can be seen from Fig. 1 that the time-delay of distributed control system is mainly composed of transmission delay and execution delay. In the process of network transmission, the delay caused by queuing and competing to use bus is called the transmission delay, and the delay caused by each intelligent node in data processing and operation tasks is called the execution delay, which is also referred to as software delay.

Total time-delay of distributed control system is described as

$$\tau = \tau_{ca} + \tau_{sc} + \tau_{a} + \tau_{s} + \tau_{c} \tag{1}$$

Where, τ is the total delay of distributed control system. τ_{ca} is the transmission delay of data from controller node to actuator node. τ_{sc} is the transmission delay of data from sensor node to controller node. τ_a, τ_c and τ_s are the execution delays of actuator node, controller node, and sensor node respectively.

The size of the execution delay is determined by the hardware and software of the system. Yu et al. [22]made an in-depth analysis of the software delay of the distributed control system, and concluded that with the condition of high-speed CPU and high-efficiency software coding, the system execution delay is about 100μs, which almost exert no influence on the performance of the control system. Therefore, the execution delay can be ignored, and the network time-delay in DCS can be simplified as follows:

$$\tau = \tau_{ca} + \tau_{sc} \tag{2}$$

2.2 Time-delay influence on aero-engine control system

Assuming that the transfer functions of the controller and the aero-engine (controlled object) in Fig. 2 are expressed as $G_c(s)$ and $G_p(s)$, respectively. Considering the time-delay τ_{ca} and τ_{sc} in formula (2), the closed-loop characteristic equation of the system can be expressed as

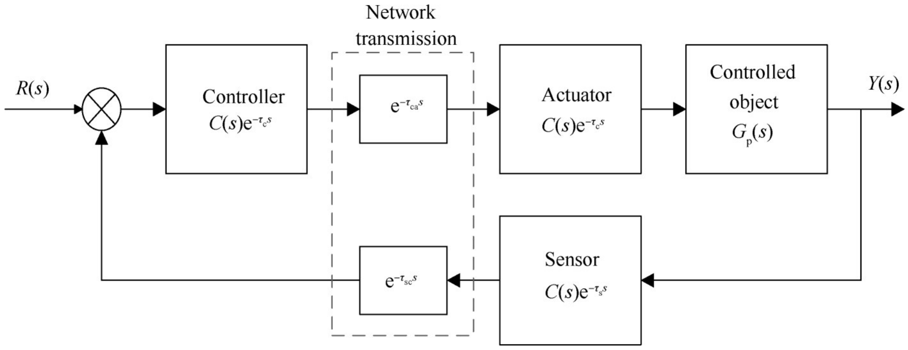

Fig. 1 Time-delay composition of typical distributed control systems

$$1+G_c(s)e^{-\tau_{ca}s}G_p(s)e^{-\tau_{sc}s}=0 \tag{3}$$

It can be seen from formula (3) that the characteristic equation contains the time-delay exponential terms of $e^{-\tau_{ca}s}$ and $e^{-\tau_{sc}s}$, which will have a great impact on the stability and control quality of the system.

In order to illustrate the effects of time-delay on the stability of the control system more intuitively, simulation examples under different cases are given below. Here the pre-designed H_∞ multi-variable control algorithm with adjusted control parameters is utilized, referred to as the traditional method.

In the first case, it is assumed that τ_{sc} is a fixed value 500ms, and τ_{ca} is changed to observe the influence of τ_{ca}. The system output curves are shown in Fig. 2. It is worth noting that the high-pressure rotor speed is the relative conversion speed and it is a dimensionless quantity, which is also applied for other figures. It can be seen that, when τ_{sc} is constant, the overshoot of the system increases with the increases of τ_{ca}, and the time required to reach stability grows accordingly. It is obvious that oscillations happen during transient state, which is not expected for the aero-engine.

In the second case, total time-delay is considered as a fixed value 1000ms, and the simulation results with different time-delay combinations are shown in Fig. 3. It is presented that, when the total time-delay is certain, the larger the value τ_{ca} is, the slower the system's dynamic response will be. Therefore, the impact of forward channel time-delay τ_{ca} on the system performance should be fully considered in the design of the aero-en-

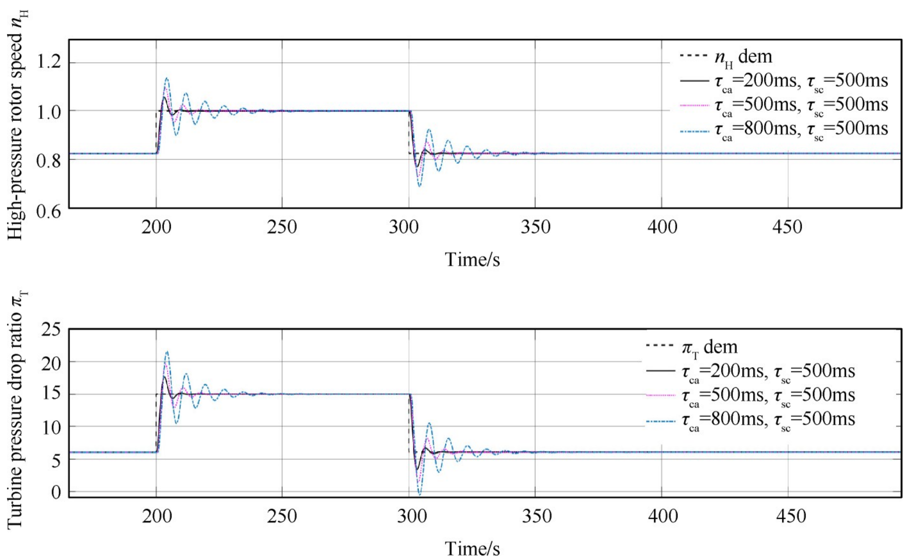

Fig. 2 Simulation examples with fixed time-delay τ_{sc}

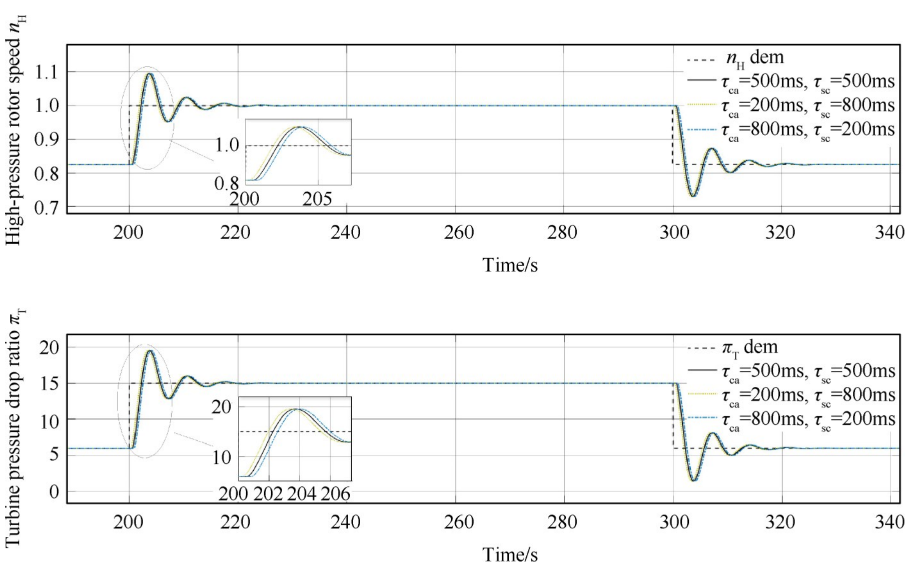

Fig. 3 Simulation examples with fixed total time-delay

gine control system.

From the above two cases, the system dynamic performance with time-delay is not satisfying under the traditional control strategy, which has large overshoot, oscillations and long settling time. So the new control strategy with time-delay should be investigated to enhance the control performance of the aero-engine.

2.3 Aero-engine internal model control structure with time-delay

In this paper, only the time-delay τ_{ca} is considered, and the structure of internal model control system with time-delay for aero-engine is shown in Fig. 4, which mainly includes a starting open-loop controller, an actuator PID controller, a switching controller and the internal model main controller.

In the proposed control scheme, the control variables are main fuel flow W_{fm} and nozzle area A_8, and the controlled variables are high-pressure rotor speed $n_H$and turbine pressure drop ratio π_T. The throttle power lever angle (PLA) is taken as the control command, and the starting threshold PLA_{st} is set as the basis for switching between the starting state and the non-starting state. When PLA is less than PLA_{st}, the engine is in starting state, and the target value of the control quantity is directly given by the open-loop controller, and when PLA is larger than PLA_{st}, the engine is at idle state or above. At this time, the system obtains the corresponding target value of high-pressure rotor speed and turbine pressure drop ratio through the interpolation table of control schedule, and then the closed-loop master controller (IMC controller) computes the control values W_{fm} and A_8.

As for the actuator part, the actuator controller receives the target values of the control quantity, calculates the PWM (Pulse-Width Modulation) signal to drive the actuator structure through PID control logic, and receives the feedback value of the actuator sensor to form an inner-loop control structure. The control period of the inner-loop control is 5ms. The aero-engine is driven by the actuator. The data of high-pressure rotor speed and turbine pressure drop ratio in the current state are collected by the speed and pressure sensors, and fed back to the main controller to form an outer-loop control loop. The control period of the outer-loop control is 10ms. At the same time, considering the high requirements of IMC controller on the accuracy of the model, the neural network time series prediction algorithm is proposed to predict the time-delay, and the predicted time-delay is sent to the IMC main controller, further optimizing the control effect.

3 Design of internal model controller based on time-delay prediction

3.1 Time-delay prediction based on neural network

BP neural network, also known as back propagation network, is a multi-layer forward network for weight training of nonlinear differentiable functions, including input layer, hidden layer and output layer. The structure diagram of typical BP neural network is shown in Fig. 5.

The nodes in BP network represent the data processing function of the current position, which is called excitation function, and the connection between nodes represents the weight of the data passing through the

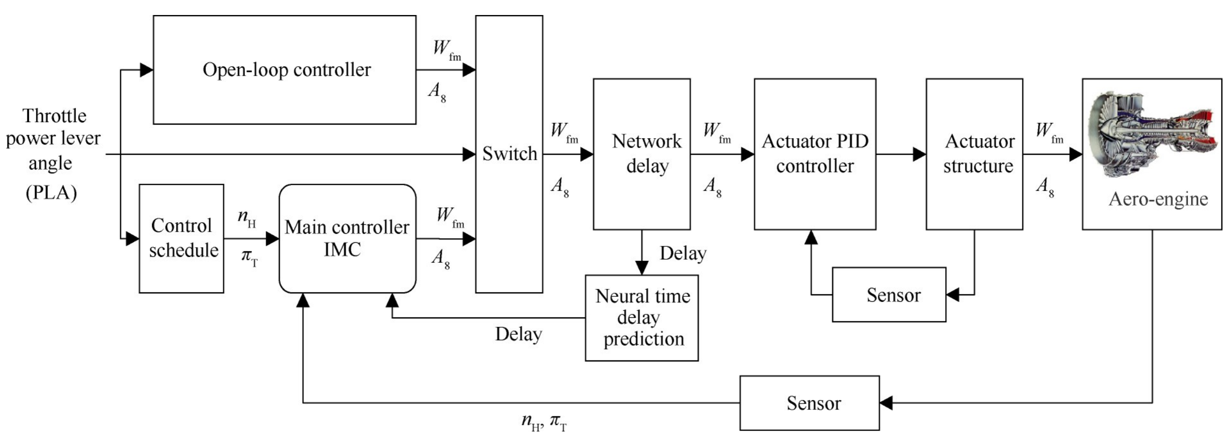

Fig. 4 Aero-engine control scheme with time-delay

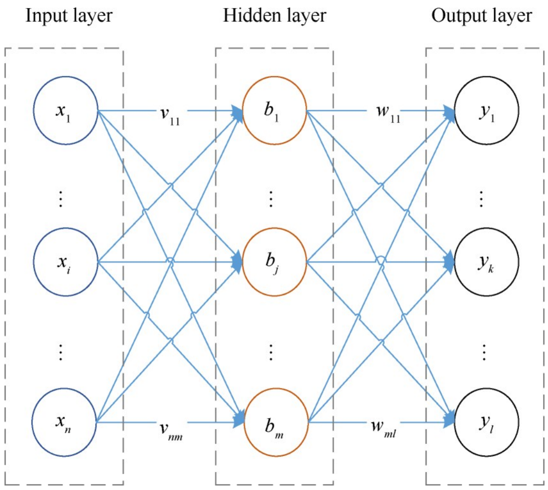

Fig. 5 Structure diagram of typical BP neural network

line. In the training process, the network can learn the data mapping relationship adaptively by modifying the weight parameters.

The construction process of BP neural network is mainly composed of forward propagation and reverse derivation. In the process of forward propagation, given the weight and threshold matrix, the predicted value corresponding to the given sample can be obtained. In the process of inverse derivation, the network parameters are constantly corrected by the error between the predicted values and the true values of the samples until convergence.

It can be seen from Fig. 5 that the input of the j^{th} neuron in the hidden layer can be expressed as

$$\alpha_j = \sum_{i=1}^{n} v_{ij} x_i \tag{4}$$

The input of the k^{th} neuron in the output layer is expressed as

$$\beta_k = \sum_{j=1}^{m} w_{jk} b_j \tag{5}$$

The nonlinear transformation function (Sigmoid function) is adopted as excitation function, namely,

$$f(x) = \frac{1}{1 + e^{-x}} \tag{6}$$

θ_j^b indicates the threshold of the j^{th} neuron in the hidden layer, and the output of the j^{th} neuron in the hidden layer is

$$b_j = f(\alpha_j - \theta_j^b) = f\left(\sum_{i=1}^{n} v_{ij} x_i - \theta_j^b\right) \tag{7}$$

The output of the k^{th} neuron in the output layer is

$$y_k = f(\beta_k - \theta_k^y) = f\left(\sum_{j=1}^{m} w_{jk} b_j - \theta_j^y\right) \tag{8}$$

Because the weights and thresholds in the forward propagation stage are randomly initialized, it is necessary to constantly modify the parameters according to the network output error. Define the error function as

$$E = \frac{1}{2} \sum_{k=1}^{l} (Y_k - y_k)^2 \tag{9}$$

Where Y_k is the target output.

Using gradient descent method and error function to calculate partial derivative of network weight, the change of output layer weight can be obtained as follows:

$$\Delta w_{jk} = \eta \delta_{jk} b_j \tag{10}$$

The variation of hidden layer weights is

$$\Delta w_{ij} = \eta \delta_{ij} x_i \tag{11}$$

Where, $\delta_{ij} = \sum_{k=0}^{l} \delta_{jk} w_{jk} x_j (1 - b_j)$, $\delta_{jk} = (Y_k - y_k) y_k (1 - y_k)$, η is the learning rate.

The weights are constantly revised and when the error is less than a certain value, the recursion is terminated, and the convergent neural network model is obtained.

According to the characteristics of network delay time series, nonlinear autoregressive (NAR) method is selected to construct neural network, and the time-delay from $k-n$ time to $k-1$ time is utilized to predict the current time-delay, namely:

$$y(k) = f(y(k-1), \cdots y(k-n)) \tag{12}$$

When n=10, the structure diagram of neural network is shown in Fig. 6. It contains an input layer node, 10 hidden layer nodes and an output node.

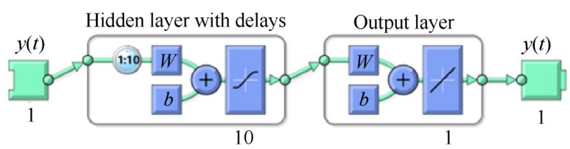

Fig. 6 Structure diagram of neural network

The training sample used in this paper is the actual time-delay data of aviation test verification platform. A total of 2500 continuous random time-delay data were collected, and the first 2000 time-delay data were taken as neural network training samples and the last 500 data were taken as test data. The data acquisition process is shown in Fig. 7.

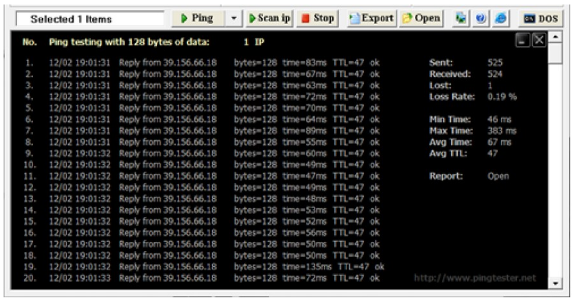

Fig. 7 Time-delay samples acquisition

Levenberg–Marquardt algorithm is used to train the neural network. The error histogram of neural network is shown in Fig. 8.

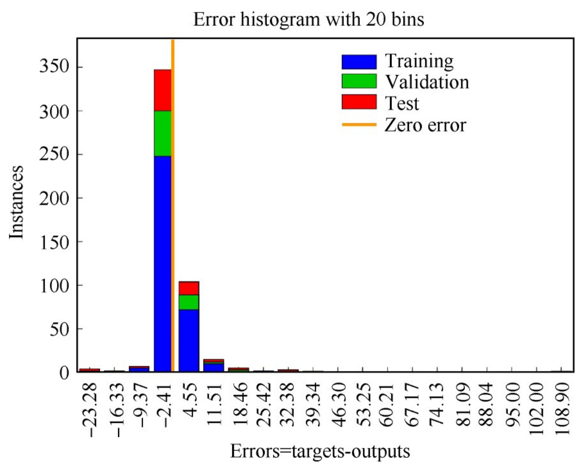

Fig. 8 Training error of neural network

3.2 IMC master controller with time–delay

3.2.1 Analysis of stability and permitted time–delay

The structure of the internal model control system with time–delay is shown in Fig. 9.

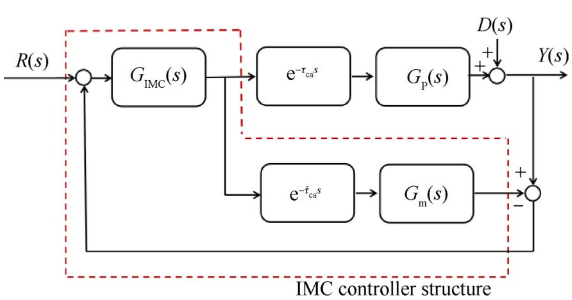

Fig. 9 IMC controller structure with time-delay

In Fig. 9, $G_{\mathrm{IMC}}(s)$ and $G_{\mathrm{p}}(s)$ represent the transfer function of internal model controller and actual controlled object respectively, $G_{\mathrm{m}}(s)$ refers to the corresponding mathematical model transfer function, and time–delay $\hat{\tau}_{\mathrm{ca}}$ means the predicted value.

The transfer function between the system output $Y(s)$ and the reference input $R(s)$ is

$$\frac{Y(s)}{R(s)}=\frac{G_{\mathrm{IMC}}(s)\mathrm{e}^{-\tau_{\mathrm{ca}}s}G_{\mathrm{p}}(s)}{1+G_{\mathrm{IMC}}(s)\left[\mathrm{e}^{-\tau_{\mathrm{ca}}s}G_{\mathrm{p}}(s)-\mathrm{e}^{-\hat{\tau}_{\mathrm{ca}}s}G_{\mathrm{m}}(s)\right]} \tag{13}$$

The transfer function between system output $Y(s)$ and interference input $D(s)$ is

$$\frac{Y(s)}{D(s)}=\frac{1-G_{\mathrm{IMC}}(s)\mathrm{e}^{-\hat{\tau}_{\mathrm{ca}}s}G_{\mathrm{m}}(s)}{1+G_{\mathrm{IMC}}(s)\left[\mathrm{e}^{-\tau_{\mathrm{ca}}s}G_{\mathrm{p}}(s)-\mathrm{e}^{-\hat{\tau}_{\mathrm{ca}}s}G_{\mathrm{m}}(s)\right]} \tag{14}$$

The output can then be expressed as

$$Y(s)=\frac{G_{\mathrm{IMC}}(s)\mathrm{e}^{-\tau_{\mathrm{ca}}s}G_{\mathrm{p}}(s)}{1+G_{\mathrm{IMC}}(s)\left[\mathrm{e}^{-\tau_{\mathrm{ca}}s}G_{\mathrm{p}}(s)-\mathrm{e}^{-\hat{\tau}_{\mathrm{ca}}s}G_{\mathrm{m}}(s)\right]}R(s)+\frac{1-G_{\mathrm{IMC}}(s)\mathrm{e}^{-\hat{\tau}_{\mathrm{ca}}s}G_{\mathrm{m}}(s)}{1+G_{\mathrm{IMC}}(s)\left[\mathrm{e}^{-\tau_{\mathrm{ca}}s}G_{\mathrm{p}}(s)-\mathrm{e}^{-\hat{\tau}_{\mathrm{ca}}s}G_{\mathrm{m}}(s)\right]}D(s) \tag{15}$$

Some assumptions are made here. The mathematical model of the controlled object can accurately restore the characteristics of the actual controlled object, that is, $G_{\mathrm{m}}(s)=G_{\mathrm{p}}(s)$. There is no interference input, that is, $D(s)=0$. The predicted time–delay $\hat{\tau}_{\mathrm{ca}}$ is equal to the real time–delay τ_{ca}. Under these conditions, the output of the system can be simplified as

$$Y(s)=G_{\mathrm{IMC}}(s)\mathrm{e}^{-\tau_{\mathrm{ca}}s}G_{\mathrm{p}}(s)R(s) \tag{16}$$

According to the dual stability of internal model control, the internal model controller can be directly constructed for the open–loop stable controlled object. However, for the open–loop unstable controlled object, it is necessary to design the stabilization system in advance. A rational internal model controller can be designed as

$$G_{\mathrm{IMC}}(s)=G_{\mathrm{p}}^{-1}(s)=G_{\mathrm{m}}^{-1}(s) \tag{17}$$

Substituting it into formula (16), then the following equation holds.

$$Y(s)=\mathrm{e}^{-\tau_{\mathrm{ca}}s}R(s) \tag{18}$$

According to the inverse Laplace transformation, the formula (18) can be converted to formula (19):

$$y(t)=r(t-\tau_{\mathrm{ca}}) \tag{19}$$

It is obvious that the output $y(t)$ has a time–delay τ_{ca} relative to the reference value $r(t)$, while the steady–state error is zero.

In practice, the interference can not be ignored. Then the error of the internal model control system can be expressed as

$$E(s)=R(s)-Y(s)=\frac{1-G_{\mathrm{IMC}}(s)\mathrm{e}^{-\hat{\tau}_{ca}s}G_{\mathrm{m}}(s)}{1+G_{\mathrm{IMC}}(s)[\mathrm{e}^{-\tau_{ca}s}G_{\mathrm{p}}(s)-\mathrm{e}^{-\hat{\tau}_{ca}s}G_{\mathrm{m}}(s)]}R(s)+\frac{1-G_{\mathrm{IMC}}(s)\mathrm{e}^{-\hat{\tau}_{ca}s}G_{\mathrm{m}}(s)}{1+G_{\mathrm{IMC}}(s)[\mathrm{e}^{-\tau_{ca}s}G_{\mathrm{p}}(s)-\mathrm{e}^{-\hat{\tau}_{ca}s}G_{\mathrm{m}}(s)]}D(s)=\frac{1-G_{\mathrm{IMC}}(s)\mathrm{e}^{-\hat{\tau}_{ca}s}G_{\mathrm{m}}(s)}{1+G_{\mathrm{IMC}}(s)[\mathrm{e}^{-\tau_{ca}s}G_{\mathrm{p}}(s)-\mathrm{e}^{-\hat{\tau}_{ca}s}G_{\mathrm{m}}(s)]}(R(s)-D(s)) \tag{20}$$

Assuming $G_{\mathrm{IMC}}(0)=G_{\mathrm{m}}^{-1}(0)$, there exist:

$$E(0)=\frac{1-G_{\mathrm{IMC}}(0)\mathrm{e}^{0}G_{\mathrm{m}}(0)}{1+G_{\mathrm{IMC}}(s)[\mathrm{e}^{0}G_{\mathrm{p}}(0)-\mathrm{e}^{0}G_{\mathrm{m}}(0)]}\cdot(R(0)-D(0))=0 \tag{21}$$

The steady-state error of the system is:

$$\mathrm{e}(\infty)=\lim_{s\to 0}sE(s)=0 \tag{22}$$

From the above deduction, it can be concluded that when there exists disturbance, as long as $G_{\mathrm{IMC}}(0)=G_{\mathrm{m}}^{-1}(0)$ is satisfied, that is, the steady-state gain of the internal model controller is equal to the reciprocal of the steady-state gain of the model, the steady-state error in the system output will be eliminated.

As for the maximum allowable time-delay τ_{ca}, from the perspective of control theory, it can be seen from formula(19) that, under the proposed IMC control strategy, the system can track the expected reference value after the delayed time τ_{ca}, no matter how large it is. However, from a practical engineering point of view, the maximum allowable time-delay depends on the maximum allowable lag time demand of the flight task to the engine response time.

3.2.2　Design process

The structure of the internal model control system with time-delay for the aero-engine is shown in Fig. 10. The aero-engine nonlinear model is treated as the actual controlled object simulator. The time-delay predicted value obtained by the neural network prediction module is taken as the internal model path delay. It is noted that in the system, the closed-loop controller of the actuator and the neural network delay prediction module, all belong to the IMC main controller.

The design process of internal model controller is mainly divided into two parts: inversion of the controlled object model and filter design. Firstly, the transfer function of the ideal internal model controller is obtained by inverting the controlled object model, and then the robustness of the system is enhanced by introducing filters.

3.2.2.1　Inversion of the controlled object model

For a certain turbofan engine, a linearized model near a typical operating point is obtained through system identification, and its state space model is shown as follows.

$$\begin{cases}\dot{x}(t)=\boldsymbol{A}x(t)+\boldsymbol{B}u(t)\\ y(t)=\boldsymbol{C}x(t)+\boldsymbol{D}u(t)\end{cases} \tag{23}$$

Where, $x(t)$ is the system state, $u(t)$ is the control input, $y(t)$ is the system output.

Then after Laplace transformation under zero initial condition, there exist:

$$G_{\mathrm{m}}(s)=\frac{Y(s)}{U(s)}=\boldsymbol{C}[s\boldsymbol{I}-\boldsymbol{A}]^{-1}\boldsymbol{B}+\boldsymbol{D} \tag{24}$$

The inversion model can then be obtained, referred to as $G_{\mathrm{m}}^{-1}(s)$.

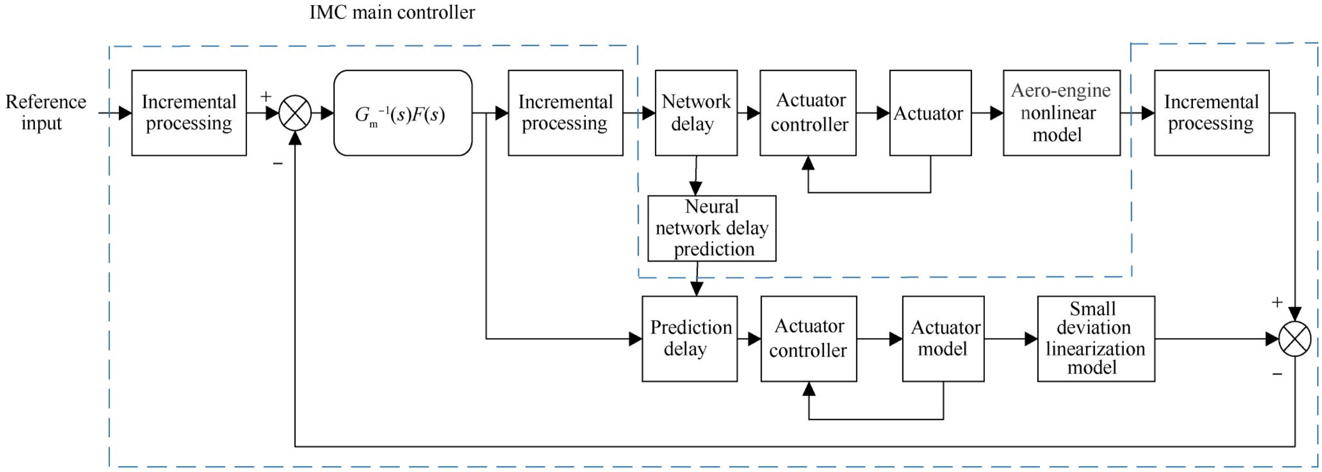

Fig. 10　Structure diagram of IMC main controller

3.2.2.2　Filter design

According to the characteristics of the turbofan engine model, I-type filter $F(s)$ is designed as

$$F(s) = \frac{1}{(T_f s + 1)^q} \tag{25}$$

Where, T_f is the filter time constant, and q is an integer that makes $G_{IMC}(s)$ a rational transfer function. If the q value is too large, it will affect the dynamic response speed of the system, while if it is too small, it will have influence on the robustness of the system. Choosing the filter parameters reasonably, the transfer function of the internal model controller is obtained as follows

$$G_{IMC}(s) = G_m^{-1}(s)F(s) = G_m^{-1}(s)\frac{1}{(T_f s + 1)^q} \tag{26}$$

4　Digital and hardware simulation verification

In this section, the control effect of the proposed IMC controller that considering time-delay is verified by digital simulation and the hardware-in-the-loop simulation test, which proves the effectiveness of the designed controller.

4.1　Digital simulation verification

The simulation model of neural network time-delay prediction module built in Simulink platform is shown in Fig. 11.

The constructed neural network module is utilized to predict the time-delay, and the predicted time-delay is compared with the actual time-delay, which is shown in Fig. 12. It can be seen that the trained neural network module owns a good prediction effect on time-delay. In addition, the predicted time-delay error is presented in Fig. 13, and it is worth noting that the predicted delay has a smaller time lag characteristic than the actual delay, so there exist large continuous deviations on the graph, whose upper and lower amplitude are close to each other.

At the ground idle state, according to formula (23), the coefficient matrices of the turbofan engine model are obtained as

$$\boldsymbol{A} = \begin{bmatrix} -2.0020 & -3.6312 \\ -0.1502 & -4.7309 \end{bmatrix} \qquad \boldsymbol{B} = \begin{bmatrix} 0.0173 & 0.0090 \\ 0.0036 & 0.0106 \end{bmatrix}$$
$$\boldsymbol{C} = \begin{bmatrix} 1 & 0 \\ 0 & 1 \end{bmatrix} \qquad \boldsymbol{D} = \begin{bmatrix} 0 & 0 \\ 0 & 0 \end{bmatrix} \tag{27}$$

And the inputs and outputs are $\boldsymbol{u} = [\Delta W_{fm} \quad \Delta A_8]$, $\boldsymbol{y} = [\Delta n_H \quad \Delta \boldsymbol{\pi}_T]^T$.

Obviously, the system can be controlled and observed. The transfer function matrix of the system is then obtained as follows:

$$\boldsymbol{G}_m(s) = \begin{bmatrix} \dfrac{0.0173s + 0.068772}{s^2 + 6.7329s + 8.9259} & \dfrac{0.0036s + 0.0046087}{s^2 + 6.7329s + 8.9259} \\ \dfrac{0.009s + 0.0040874}{s^2 + 6.7329s + 8.9259} & \dfrac{0.0106s + 0.019869}{s^2 + 6.7329s + 8.9259} \end{bmatrix} \tag{28}$$

There does not exist non-minimum phase part in the model, so its inverse matrix $\boldsymbol{G}_m^{-1}(s)$ can be directly computed.

According to formula (25), parameters T_f=0.5 and q=2 are set, and I-type filter $F(s)$ is then designed .The transfer function of the internal model controller can be obtained as

$$\boldsymbol{G}_{IMC}(s) = \boldsymbol{G}_m^{-1}(s)F(s) = \boldsymbol{G}_m^{-1}(s)\frac{1}{(0.5s + 1)^2} \tag{29}$$

According to the method given in Section 3, the IMC control system with time-delay is built in Simulink platform. The response curves of the high-pressure rotor speed n_H and the turbine pressure drop ratio $\boldsymbol{\pi}_T$ are obtained, as shown in Fig. 14. It can be seen that there is almost no difference between the output responses under

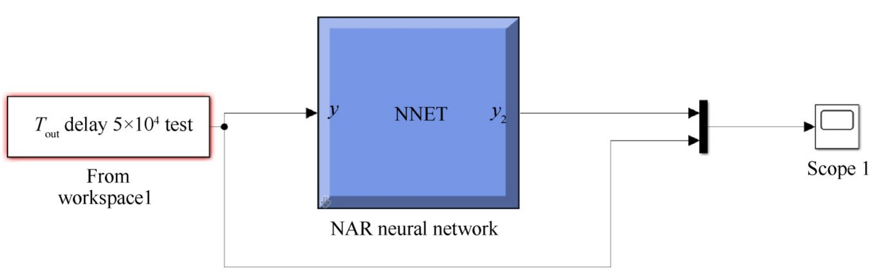

Fig. 11　Neural network prediction module built in Simulink platform

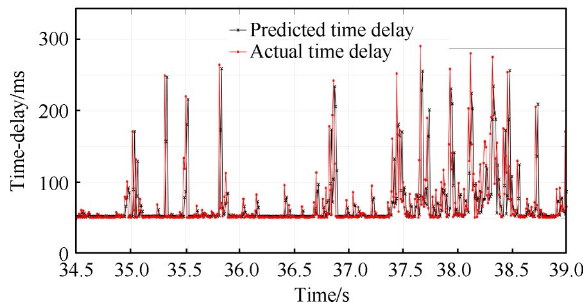

Fig. 12　Time-delay prediction effect based on neural network

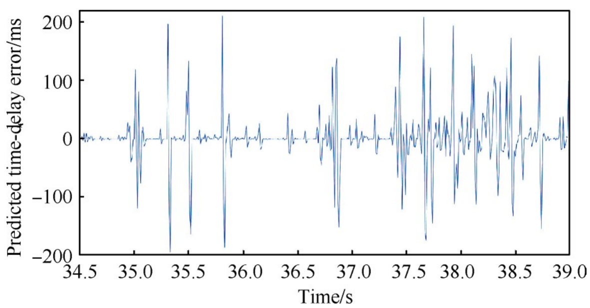

Fig. 13　Time-delay prediction error based on neural network

the conditions of actual delay and predicted delay, which also proves the accuracy of the constructed neural network delay prediction module.

In addition, the controller is simulated and verified under the time-delay of 180ms, 400ms, 600ms and 5s. The control effect of IMC controller under different time-delay is shown in Fig. 15. It can be observed that the output response curves only translate along the time axis with the increase of time-delay, which is consistent with the formula (19). Even under the long delay of 5s, there is no oscillation phenomenon, and the dynamic response is also good. The adjustment time is less than 5s, the steady-state error is less than 0.5%, and the overshoot is less than 5%.It can be concluded that IMC controller has a very satisfactory control effect on any time-delay under the premise of high model accuracy.

Fig. 16 shows the system response with different levels of sinusoidal interference. Under the condition of 180ms delay, and when 0.1% white noise is added to the feedback channel, it has little effect on the stability of the system. When 1% noise is considered, the output of the turbine pressure drop ratio oscillates slightly, but it can still follow the given value and maintain the system performance. The results show that the designed IMC controller owns good anti-noise ability.

4.2　Hardware-in-the-loop simulation verification

Aero-engine hardware-in-the-loop test platform can be utilized to simulate the working states under the whole flight envelope. Through the combination of software and hardware of the system, it simulates the input and feedback signals of sensors, actuators and other devices during the engine starting, idling and cruising states, and the digital electronic controller (EEC) executes the control algorithms to form the FADEC control loop, thus realizing the hardware-in-the-loop simulation verification of the aero-engine control algorithms.

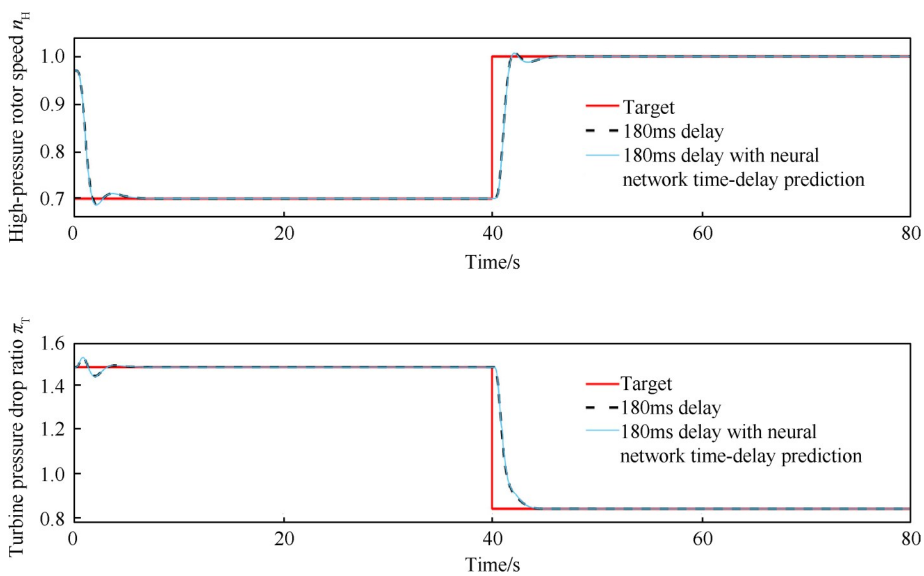

Fig. 14　Control effect of IMC with neural network time-delay prediction

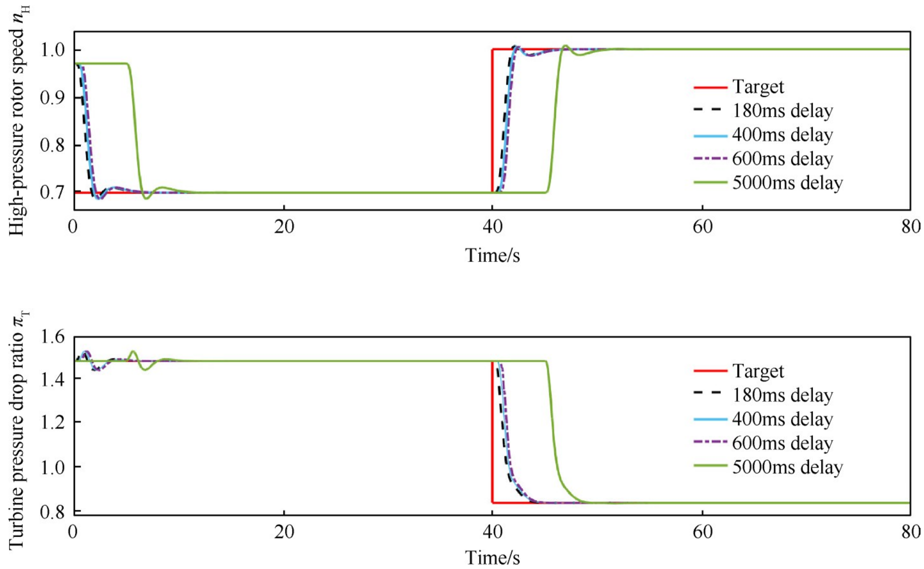

Fig. 15 Control effect of IMC with different time-delay

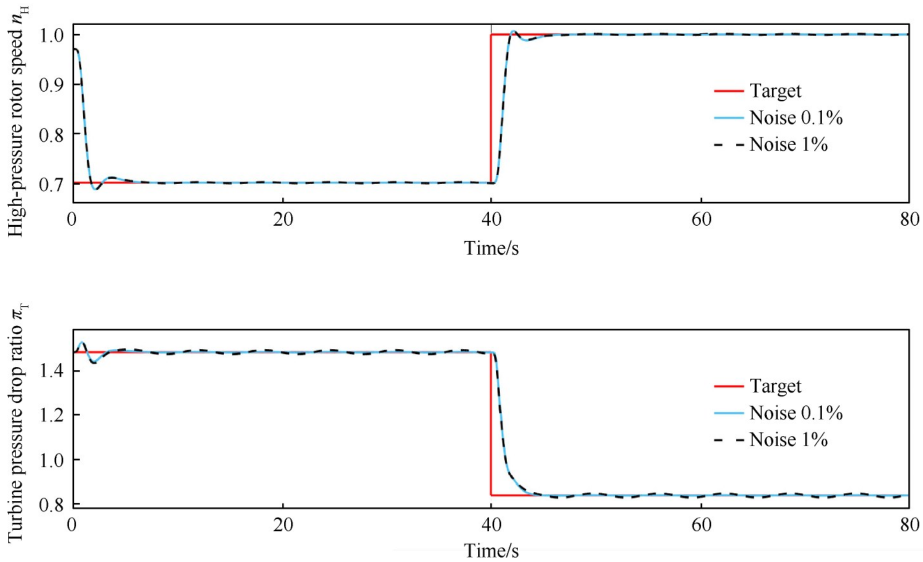

Fig. 16 Control effect of IMC with different noise levels

On the hardware-in-the-loop simulation platform, the closed-loop simulation test of the designed IMC time-delay control system at nominal state is carried out. The Simulink model of the controller is converted into C code and downloaded to the digital electronic controller. The engine is controlled to start by pushing the throttle lever angle PLA command, and then transits to the idle state and switches to the IMC main controller mode. The response curve comparisons between hardware-in-the-loop (HIL) simulation results and pure digital simulation (SIL) results of engine at idle and above states are shown in Fig. 17.

It can be seen that the hardware-in-the-loop simulation results are basically consistent with the pure digital simulation results, and the dynamic performance is satisfying. The adjustment time during the large transition state is less than 10s, and there is no obvious steady-state error. Due to the characteristics of the engine, the turbine pressure drop ratio loop has some overshoot, but it does not affect the system stability, and this is permitted in the practice engineering application.

The hardware-in-the-loop test results indicate that the IMC control method that designed in this paper can meet the real-time requirements and has the feasibility of engineering application.

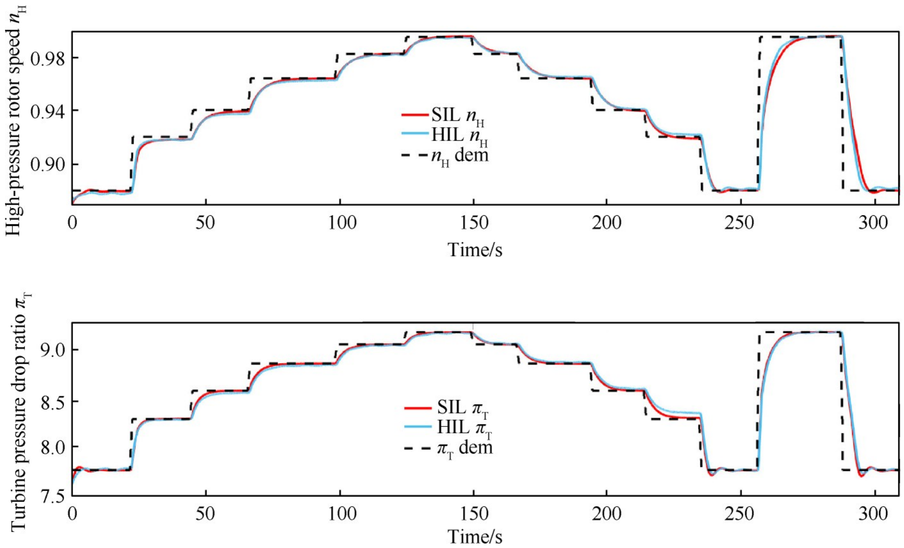

Fig. 17 Simulation results of IMC on hardware-in-the-loop platform

5 Conclusion

An internal model controller based on neural network time-delay prediction is designed for a turbofan engine, some conclusions can be obtained through theoretical analysis and simulation verification.

(1) When conventional H_∞ multi-variable control algorithm of the turbofan engine is adopted, the long time-delay could result in the fluctuations of key performance parameters during transient state, thus influencing the system stability. The results show that the proposed neural network internal model control strategy has remarkable control effect on ultra-long time-delay, achieving satisfactory dynamic and static response, and owns strong anti-interference ability.

(2) Theoretically, under ideal conditions, that is, there is no model mismatch and the time-delay prediction is accurate, the proposed control strategy can handle arbitrary long time-delay, and the system response is postponed by the corresponding time-delay quantitative value. The maximum allowable time-delay is governed only by the lag time that the engine response is permitted by the aircraft.

(3) The designed internal model controller can generate embedded code and operate in the digital electronic controller of the hardware-in-the-loop platform, which indicates that the proposed strategy meets the real-time requirements.

Acknowledgement: This work is supported by National Natural Science Foundation (NNSF) of China, Aviation Science Foundation of China, Liaoning Revitalization Talents Program, the Fundamental Research Funds for the Central Universities and National Science and Technology Major Project.

References

[1] Timothy M S, Qwen B M, Alireza R B, et al. Development of Distributed Control Systems for Aircraft Turbofan Engines[R]. *AIAA* 2016-4805.

[2] Du L, Guo Y, Zhan H, et al. Research on Key Technologies of Multi-Smart-Agents Based Partially Distributed Control System for Aero Engine[C]. *Tokyo: 6th IFAC Conference on Engine Powertrain Control, Simulation and Modeling E-COSM* 2021, 2021.

[3] 徐若淞，谢寿生，李腾辉，等．基于多模型切换的航空发动机分布式鲁棒跟踪控制器设计[J]．推进技术，2019，40(12)：2837-2847.（XU Ruo-song, XIE Shou-sheng, LI Teng-hui, et al. Design of Distributed Robust Tracking Controller for Aeroengine Based on Multiple Model Switching[J]. *Journal of Propulsion Technology*, 2019, 40(12): 2837-2847.）

[4] Lavault C. Average Number of Messages for Distributed Leader Finding in Rings of Processors[C]. *Paderborn: Annual Symposium on Theoretical Aspects of Computer Science*, 1989.

[5] Luo H, Hu Z. Stability Analysis of Sampled-Data Control Systems with Multiple Time-Varying Delays[J]. *Journal of the Franklin Institute*, 2020, 357(11): 6615-6634.

[6] Mulay S P, Yedavalli R K. Robust Stability of Uncertain Sampled Data Time Delay Systems with Application to

Turbine Engine Control[C]. *Boston*: *AIAA Guidance*, *Navigation*, *& Control*, 2013.

[7] Belapurkar K R, Yedavalli K R, Moslehi B. Stability of Fiber Optic Networked Decentralized Distributed Engine Control under Time Delays[C]. *Denver*: 45*th AIAA/ASME/SAE/ASEE Joint Propulsion Conference and Exhibit*, 2009.

[8] Yedavalli R K, Belapurkar R K, Behbahani A. Design of Distributed Engine Control Systems for Stability under Communication Packet Dropouts[J]. *Journal of Guidance*, *Control*, *and Dynamics*, 2009, 32(5): 1544-1549.

[9] Yedavalli K R, Belapurkar K R, Behbahani A. Stability Analysis of Distributed Engine Control Systems under Communication Packet Drop[C]. *Hartford*: 44*th AIAA/ASME/SAE/ASEE Joint Propulsion Conference and Exhibit*, 2008.

[10] Kratz J L, Yedavalli R K, Behbahani A R. A Riccati Equation Based Robust Control Design with Application to a Gas Turbine Engine Leading Toward Distributed Control[C]. *Cleveland*: 50*th AIAA/ASME/SAE/ASEE Joint Propulsion Conference*, 2014.

[11] Jonathan D, Liang T, Carl B, et al. Analysis of Decentralization and Fault-Tolerance Concepts for Distributed Engine Control[C]. *Denver*: 45*th AIAA/ASME/SAE/ASEE Joint Propulsion Conference and Exhibit*, 2009.

[12] Belapurkar K R, Yedavalli K R, Paul P, et al. Stability Analysis of ARINC 825-b Based Partially Distributed Aircraft Engine Control with Transmission Delays and Packet Dropouts[C]. *Nashville*: 46*th AIAA/ASME/SAE/ASEE Joint Propulsion Conference and Exhibit*, 2010.

[13] Seitz T M, Yedavalli R K, Macmann O, et al. Robust Control of Turbine Engines Using Distributed Networks with Multiple Time Delays[J]. *Journal of Guidance*, *Control*, *and Dynamics*, 2017, 40(11): 2771-2781.

[14] Chen Y, Guo Y, Li R. State Feedback Control for Partially Distributed Turboshaft Engine with Time Delay and Packet Droputs[C]. *Wuhan*: 37*th Chinese Control Conference*(*CCC*), 2018.

[15] Li Jiejie, Du Xian, Sun Ximing, et al. Improved Smith Predictive Control Design of Aeroengine Based on H_∞ Algorithm[C]. *Shenyang*: *Proceedings of the* 39*th Chinese Control Conference*, 2020.

[16] Garcia C E, Morari M. Internal Model Control. 1. A Unifying Review and Some New Results[J]. *Industrial & Engineering Chemistry Process Design and Development*, 1982, 21(2): 308-323.

[17] Anwar M N, Pan S, Raza A. PID Controller Tuning in Smith Predictor Configuration for Stable Processes with Large Time Delay Using IMC Scheme[C]. *Jharkhand*: 2017 *International Conference on Energy*, *Materials and Information Technology*, 2017.

[18] Kumar M, Prasad D, Singh R S. Performance Enhancement of IMC-PID Controller Design for Stable and Unstable Second-Order Time Delay Processes[J]. *Journal of Central South University*, 2020, 27(1): 88-100.

[19] Giorgi M, Quarta M. Hybrid Multigene Genetic Programming-Artificial Neural Networks Approach for Dynamic Performance Prediction of an Aeroengine[J]. *Aerospace Science and Technology*, 2020, 103: 105902.

[20] Izzo D, Tailor D, Vasileiou T. On the Stability Analysis of Deep Neural Network Representations of an Optimal State Feedback[J]. *IEEE Transactions on Aerospace and Electronic Systems*, 2021, 57(1): 145-154.

[21] Hou Y, Chen Y, Li Q, et al. New Results on Deterministic Networked Supervisory Control and Relative Delay Observability[J]. *IEEE Access*, 2021, 9: 2032-2043.

[22] Yu H, Huang J. Analysis of the Time-Delay of Aeroengine Distributed Control System[J]. *Measurement & Control Technology*, 2008(6): 50-51.

（编辑：刘萝威）